G02

EXPERIMENTAL TECHNIQUES TO ESTIMATE TEMPERATURE FIELD AND HEAT SOURCE IN A WELDING PROCESS

C. V. Gonçalves[1], L. O. Vilarinho[2] and G. Guimarães[3]
Federal University of Uberlândia, School of Mechanical Engineering, Campus Santa Mônica,
Blc. M, 38400-902, Av. João Naves de Ávila, S/N, Uberlândia, MG, Brazil
[1]cgoncalves@mecanica.ufu.br, [2] vilarinho@mecanica.ufubr, [3] gguima@mecanica.ufu.br

Abstract - This work presents the comparison between two experimental techniques to study the thermal problem that occurs in the base material due to the welding process. The techniques combine optimization techniques such as the Simulated Annealing (SA) and the Gold Section in two different physical models. The first thermal model considers a quasi-stationary heat conduction in the interior of the material, whereas the second uses the general transient equation of heat diffusion with phase change. In both cases, the heat input generated by the welding process is estimated. However, the use of the SA techniques with the numerical model allows, additionally, the weld pool geometry identification. The inverse technique demands measurements from thermocouples placed in the opposite side to a GTAW (Tungsten Inert Gas) welding processes that is applied on a stainless steel AISI 304 plate.

1. INTRODUCTION

Welding processes that involve material phase change are used in a large number of metallic structures such as buses, airplanes, reactors or oil ducts. Once these structures have acquired a high level of safety, the manufacturing processes, in special welding, must be carefully considered. GTAW (Gas Tungsten Arc Welding) is one of the most widely employed welding processes that is applied with success for welding of stainless steels and non-ferrous materials. In this process, a tungsten electrode is shielded by a flow of inert gas such as argon (normally employed), helium, nitrogen, hydrogen or mixtures. The union of two or more workpieces is obtained through a voltaic arc which is a moving intense heat source.

The analysis of the thermal behavior of the physical phenomenon that takes place in the process is crucial to understand, for example, the width and depth of weld penetration, the microstructure changes in the base metal thermally affected or the residual stress that appear in the welding process. Also, the intensity of the heat input and the temperature gradients in the workpiece are extremely important for welding process studies. The rate between the effective heat delivered to the workpiece and electric power consumed by the power source is a good indicative of the process performance.

It can be observed [18] that not all the total electrical power necessary for obtaining the voltaic arc (voltage versus current) is absorbed by the workpiece. The difference is due to the heat losses to the environment by convection or radiation or by Joule effect in the electrode. Thus, the task is how to calculate the heat input to the workpiece and consequently the thermal efficiency. From literature, it is possible to distinguish two lines of research: one where the welding is carried out on water cooled anode and other where weldments are made on real welding conditions, i.e., without and with phase change respectively. Results published so far indicate that these two approaches of heat input calculation lead to different results. The cooled anode approach provides values of thermal efficiency of the order of 80%, whereas thermal efficiency from real weldments is of the order of 60%. This difference (~20%) is due to the latent heat, i.e., the fraction of the heat input that is not converted in temperature increase, but only in phase change.

Alternatively to these methods, the inverse heat conduction problem represents, in this case, an alternative way to obtain the heat input that goes to the workpiece. This procedure is justified by the difficulties to obtain measurements in the thermally affected zone in the weld area. The great advantage of inverse technique is the chance of obtaining the heat imposed in the weld face of the workpiece using just temperatures measured on the opposite face to the weld bead.

One requisite to determine the temperature field in the presence of welding process is to know the real heat waste or the geometry and interface position of weld pool present in the process. Once known these parameters, a direct problem is established and the temperature field can, then, be calculated. Several analytical [7, 13, 15, 18, 21, 23] or numerical [6, 10, 14, 27] works that deals with this direct problem can be found in the literature. Beside the hypothesis of knowing heat input, important phenomena like phase change, thermal properties changing with temperature or heat losses by convection or radiation are neglected or considered known [1, 8-9, 22, 26,]. However the identification of heat input or the weld pool geometry is not trivial in a real welding and must be calculated. The main difficulty, in this case, is that these parameters are available and cannot be measured directly. As mentioned, one way to avoid this difficulty is to use inverse techniques. The majority of

works that deal with application of inverse problem techniques in welding problems [2,12,19] just use simulated studies. Thus, the main goal of this work is to obtain a thermal solution of a welding problem that appears during a real GTA welding process of austenitic stainless steel AISI 304 by using inverse techniques.

2. PHYSICAL MODELS FOR GTA WELDING PROCESS

In order to develop the inverse algorithm, two theoretical models are used to solve the direct problem: a simplified two-dimensional physical model based on quasi-stationary Rosenthal's equation [1] and a transient two-dimensional physical model based on the work of Al- Khalidy [1]. On the contrast of model 1, the transient model takes into account the phase change, thermal properties changing with temperature and heat losses by convection and radiation.

2.1. Rosenthal model (model 1)

Rosenthal proposed solutions to the heat flux equation of a moving point heat-source in 1941 [1]. In his model it is assumed that the heat source moves with a constant speed u along the x-axis of a fixed rectangular co-ordinate system, as shown in Figure 1.
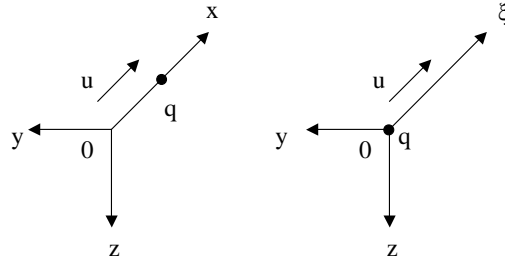

Figure 1. A moving point heat source: a) fixed coordinates x,y,z: b) moving coordinates ξ,y,z [16].

Considering Figure 1, the general energy equation for an isotropic and homogenous material, with constant properties, is reduced to:

$$\frac{\partial^2 T}{\partial x^2} + \frac{\partial^2 T}{\partial y^2} + \frac{\partial^2 T}{\partial z^2} = \frac{1}{\alpha}\frac{\partial T}{\partial t} \tag{1}$$

where α is the thermal diffusivity and x, y, z is the fixed coordinate system. If a moving point heat source (q) traveling with a constant velocity (u) in the x direction (Fig. 1) is assigned to the origin of a moving coordinate system ξ, y, z, then the transformation of a point $P(x, y, z, t)$ in the fixed system by $\xi = x - u\,t$ becomes $P(\xi, y, z)$ in the moving system [16].

The transformed form of eqn.(1) then becomes:

$$\frac{\partial^2 T}{\partial \xi^2} + \frac{\partial^2 T}{\partial y^2} + \frac{\partial^2 T}{\partial z^2} = \left(\frac{1}{\alpha}\frac{\partial T}{\partial t}\right) - \left(\frac{u}{\alpha}\frac{\partial T}{\partial \xi}\right) \tag{2}$$

Assuming that the workpiece is long enough, in such a way that the quasi-stationary condition can be established, eqn.(2) reduces to :

$$\frac{\partial^2 T(\xi, y, z)}{\partial \xi^2} + \frac{\partial^2 T(\xi, y, z)}{\partial y^2} + \frac{\partial^2 T(\xi, y, z)}{\partial z^2} = -\frac{u}{\alpha}\frac{\partial T(\xi, y, z)}{\partial \xi} \tag{3}$$

Equation (3) can be solved using the separation of variables method, taking a solution of the form as follows:

$$T(\xi, y, z) = T_0 + \frac{q}{2\pi k\delta}\exp\left(-\frac{u\xi}{2\alpha}\right)\cdot K_0\left(\frac{ur}{2\alpha}\right) \tag{4}$$

where, q is the heat, δ is the thickness K_0 is the modified Bessel function of the first kind of order zero and $r = \left(\xi^2 + y^2 + z^2\right)^{1/2}$.

The assumptions involved with eqn.(4) include a quasi-steady condition in the workpiece, the arc is represented by a point source, thermal properties are considered constant with temperature and the heat loss from the plate due to convection or radiation or phase change are neglected.

If the value of the heat input, q, is known, eqn.(4) represents the solution of the direct problem related to the inverse problem studied.

2.2. Physical model considering phase change (model 2)

Transient heat transfer problems involving melting or solidification, such as is the problem due to a GTA welding process, are usually referred to as phase-change or moving-boundary problems. The solution of such

problems is inherently difficult because the interface between the solid and liquid phases is moving as the latent heat is absorbed or released at the interface. As a result, the location of the solid-liquid interface is not known a priory and must follow as a part of the solution [24]. In the welding process, the thermal problem is, then, established when the molten pool is formed as the result of the heat source moving with a constant speed. The physical model to solve the direct problem related to phase change presented here is based on a previous work of Al-Khalidy [1] that considers a two-dimensional system and nonlinear temperature-dependent thermal conductivity $k(\theta)$ and specific heat $c(\theta)$ in the solid region.

The theoretical model developed in Ref. [1] is based on the governing equation

$$\rho C(\theta)\frac{\partial \theta(x,y,t)}{\partial t} + \rho C(\theta)\, u\, \frac{\partial \theta(x,y,t)}{\partial x} = \nabla.\left(k(\theta)\nabla \theta(x,y,t)\right) - \frac{h(\theta)}{\delta}\theta(x,y,t) + Q(\theta)_m \tag{5a}$$

where $(x,y) \in R_s \bigcup R_l = R$ is the region of pure material separated into liquid region R_l and solid region R_s. The two regions are separated by an interface $\Re$. The Equation (5a) is subjected to the boundary conditions

$$\frac{\partial \theta_l}{\partial y} = 0; \qquad \frac{\partial \theta_s}{\partial y} = 0; \quad \text{at y=0} \tag{5b}$$

$$\theta_s(x,y,t) = 0 \qquad\qquad \text{as } x \to \infty \text{ or } y \to \infty \tag{5c}$$

and initial condition

$$\theta(x,y,0) = 0 \qquad\qquad \text{for } (x,y) \in R \tag{5d}$$

In eqn.(5a) the phase change is isolated in a latent heat source term as

$$Q(\theta)_m = -\rho \frac{\partial\left(\Delta H(\theta)\right)}{\partial t} \tag{5.e}$$

and the $h(\theta)$ is the overall convective heat transfer that is calculated as $h(\theta) = h_c + h_r$, where h_r and h_c are the radiative and the convective heat transfer coefficient, respectively.

Additionally the interface condition include the isothermal condition

$$\theta_m(x,y,t) = T_m - T_\infty \qquad \text{to } (x,y) \in \Re \tag{5f}$$

If the parameters $Q(\theta)_m$ and the weld pool geometry are known, the numerical solution of eqn.(5) represents the solution of the direct problem related to the inverse problem studied. To obtain the numerical solution of eqn.(5) the finite volume method [17] is used with a grid of 360 x 90 volumes.

3. INVERSE PROCEDURE

Besides the experimental data and physical models, two techniques of optimization are also used to solve the inverse algorithm. The techniques are the simulated annealing, SA [20], and the golden section method [24]. Both, physical models and optimization techniques are used over the same experimental temperature data and this allows a good comparison of results.

3.1. *Heat estimation, q, by using simulated annealing techniques (model 1)*

One way to estimate the heat input q, present in Eq. (4), is to require that the traditional least square function, F_q, defined as the error between the computed temperature T_i and the measured temperature Y_i be minimized with respect to unknown q. F_q is then defined as

$$F_q = \sum_{i=1}^{M}\left(Y_i(\xi,y) - T_i(\xi,y,q)\right)^2 \tag{6}$$

were *i* represents the index for the thermocouple position and we have dropped the z-dependence.

There are several inverse techniques besides of SA that can solve this welding problem optimization. It can be cited, for example, the conjugate gradient with adjoint equation method [3], parameter estimation approach [4] and sequential time domain [5]. These methods use temperature histories experimentally determined in the sample (workpiece) to calculate the corresponding heat input for a given set of system parameters (welding). The SA was chosen here due, mainly, to its robust characteristic [20]. Simulated Annealing can be performed in optimization by randomly perturbing the decision variable and keeping track of the best objective function value for each randomized set of variables. After many trials, the set that produced the best objective function value is designed to be the center, over which perturbation will take place for the next temperature. The temperature, that in this technique is the standard deviation of the random number generator, is then reduced, and new trials performed.

Temperature T_i is calculated from the eqn.(4), and Y_i represents the experimental temperature measured on the opposite face to the weld bead. The iterative computational procedure to estimate the heat input q can be summarized as follow:

step 1: To start the iterations an initial estimate is made for the heat input q, which can be chosen as constant, say close to zero.

step 2: Compute $T(\xi, ,y)$ using eqn.(4).

step 3: Assuming that the search region to the optimal value of heat input, q, is between the lower bound zero and the upper bound given by the power P supplied by the GTA torch (voltage versus current) the optimization of F_q goes until the optimized value of q is found (or a stopping criterion is satisfied). Here, the criterion is $F_q < 1$ K^2.

3.2. Molten pool radius and interface position estimation (model 2)

The use of model 2 requires a new objective function. In this case, once the model is transient and the location of the phase-changing is unknown the new objective function is defined as

$$F_r = \sum_{i=1}^{N} \left(Y_i(\xi, y, t) - T_i(\xi, y, t, r) \right)^2 \tag{7}$$

where i represents the time index, r is the molten pool radius, and T represents the temperature that now is calculated from the numerical solution of eqns.(5). The inverse procedure presented by Al-Khalidy [2] for a quasi-static model is adapted here to the transient model. In contrast to that work, here the molten pool shape is assumed circular and the objective of the inverse procedure is to estimate the radius of the weld pool as well as the temperature field within the solid region. The inverse procedure, here, is stated as an optimization problem to minimize the function given by Eq.(7). The iterative computational procedure to estimate the radius, r, can be, then, summarized as follow:

step 1. Assume an arbitrary value to the radius r of the weld pool.

step 2. Assume the initial values of $\Delta H(\xi, y,t) = \Delta H_0(\xi, y, t) = 0$.

step 3. The nonlinear simultaneous set of equations, eqn.(5) is solved to determine $T(\xi, y, t)$.

step 4. Optimize the results with respect to the eqn.(7). At this step the finite volumes where the phase change occurs are identified using the optimal r value.

step 5. The steps 3 to 4 are repeated until convergence is reached.

step 6. The known values of the temperatures $T(\xi, y, t)$ and $\Delta H(\xi, y ,t)$ at any time are assumed to be the previous value in the next time step.

step 7. The calculation procedure for the new time step is repeated.

Since the optimization procedure requires the numerical solution of eqn.(5) repeated many times, the use of simulated annealing technique here could waste so much time of computing. Instead, as we have only one variable to estimate, the radius r, the golden section method is chosen to minimize the eqn.(7). The golden section method for estimating the minimum of a one-variable function is a popular technique since F_r does not need to have continuous derivatives, is easily programmed and is found to be reliable for poorly conditioned problems, see [24] for more details.

4. EXPERIMENTAL PROCEDURE

Figure 2 represents the welding rig used in the experimental procedure. The welding torch, which represents the point heat source, moves at a specific speed along a straight path by using a totally automated X-Y coordinate table. To avoid test-plate dimension interference, the test-plate is held in air by 4 pointed cylindrical screws, so that, only a small contact area exists.

A set of experiments for the AISI 304 sample with dimensions of 200x50x4 mm was made using the following welding conditions: direct polarity (CC-), voltage of 15V, current (78 A), arc length (4 mm), shielding gas (Ar and Ar+25%He) and included electrode angle (60°). The electrode used is AWS EWTh-2, tungsten doped with 2% of thory with 1.6 mm of diameter. The shielding gas flow was set at 8 l/min ($0.133\ 10^{-3}$ m/s) and the welding speed at 0.00833m/s. The values of the thermal properties of AISI 304 are obtained from literature [1]: k = 14.42 + 0.0169T – 2.44x10^{-06} T^2 [W/mK] and c_p = 486.6 + 0.159T + 18.07x10^{-06} T^2 [J/(kgK)], T_m=1700[K], and

$$h = 1.32 \left(\frac{T}{\delta} \right)^{0.25} + 0.61 \left(\frac{T}{\delta} \right)^{0.2} + 5.67 10^{-8}\ 0.95 \left(T^2 + T_\infty^2 \right) \left(T - T_\infty \right) \tag{8a}$$

if $Gr\, Pr \leq 10^9$, or

$$h = 1.32 \left(\frac{T}{\delta} \right)^{0.25} + 1.43 \left(\frac{T}{\delta} \right)^{0.333} + 5.67 10^{-8}\ 0.95 \left(T^2 + T_\infty^2 \right) \left(T - T_\infty \right) \tag{8b}$$

if $Gr\, Pr > 10^9$, were Gr and Pr are the Grashof and Prandtl number, respectively.

Capacitor discharge is used to attach the thermocouples to the plate surface. Twelve thermocouples, type K, are attached to the bottom face of the test-plate (AISI 304), Figure 2b. A well-detailed description can be found

in Vilarinho [25]. It should be observed that just four thermocouple are effectively used in the optimization process. The remaining thermocouple had been used to analysis and verify simplifying hypothesis. Figure 3 presents in detail the thermocouple location in the sample of these four thermocouples.

a)   b)

Figure 2. Experimental apparatus: a) view of welding torch; b) view of thermocouple attaching.

The welding is carried out on a plane position with the bead on plate technique. Two independent data acquisition systems are used. In the first one, a data acquisition chart is used to measure the voltage and current signals with 12 bits and 10 kHz per channel. The second one is composed by a microcomputer-based data acquisition system (HP 75000 B E1326B), DAS for short, is used in order to acquire and storage the thermocouple data. The DAS, under a software control, sampled (multiplexed) each thermocouple signal at intervals of 0.38 s (totaling 1028 points for each thermocouple).
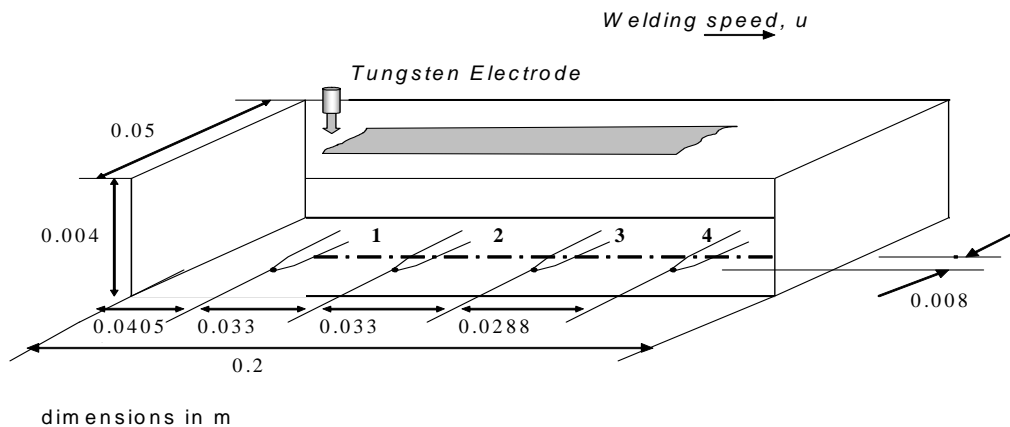

Figure 3. Thermocouple locations at opposite face of the test.

The hypotheses of infinite plate used in both physical models and the two-dimensional heat transfer (model 2) must be assured. In this sense, the experiment must be designed, such as the test plate geometry have the minimum size to attend these conditions. For verifying the infinite assumption an analysis of the 3D Rosenthal model has been performed. It can be observed that a sample width of 0.05 m is wide enough for obtaining values of temperature close to the environment temperature 300K (infinite condition). These results can been found in Ref.[11].

Another physical effect that can occur is the influence, in the temperature field, of the molten pool along the thickness direction. It means, since the two-dimensional numerical model is used, no change in temperature in the direction of thickness is expected. The way to alleviate this difficulty is to place thermocouple away of influence of the thermal resistance of weld pool. These locations, in this work, are chosen to be 0.008 m away from the symmetry line in which the torch is applied, as shown in Figure 3.

This influence is estimated through a solution of 3D numerical heat transfer diffusion with a heat source moving. The heat-moving source is used here to simulate the phase change presence in the symmetry line. This source must be supplying heat enough to allow the sample reaching a temperature high enough at fusion level. Since the model is three-dimensional any variation along the thickness can be felt. Due to the space limitations, these results that can be found in [11] are omitted here. It can be seen that 8mm is sufficient to obtain the same temperature in plane along the thickness.

5. RESULTS AND DISCUSSION

5.1. *Input data*

Figure 4 shows the measured temperatures at the bottom surface of the test-plate for the four thermocouples shown in Figure 3. From these temperatures and the choice of model the heat input, q, or the weld pool radius, r, can be obtained.
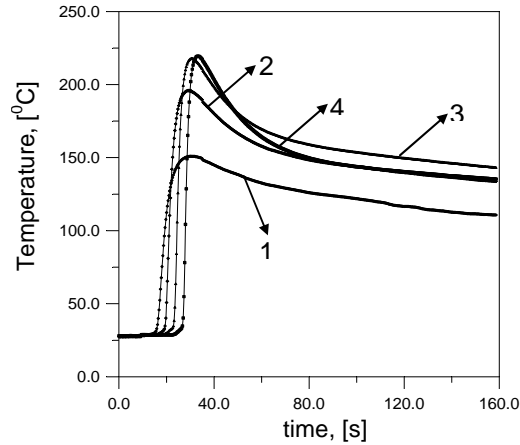

Figure 4. Measured temperatures at the bottom surface of the test-plate for the four thermocouples, shown in Figure 3.

5.2. *Temperature field and heat input estimation, q, (model 1)*

Once the heat input to the workpiece is estimated, the temperature distribution can then be obtained from eqn.(4). Figure 5 presents examples of temperature evolution estimated at four different times $t = 2, 10, 20$ and 25s.
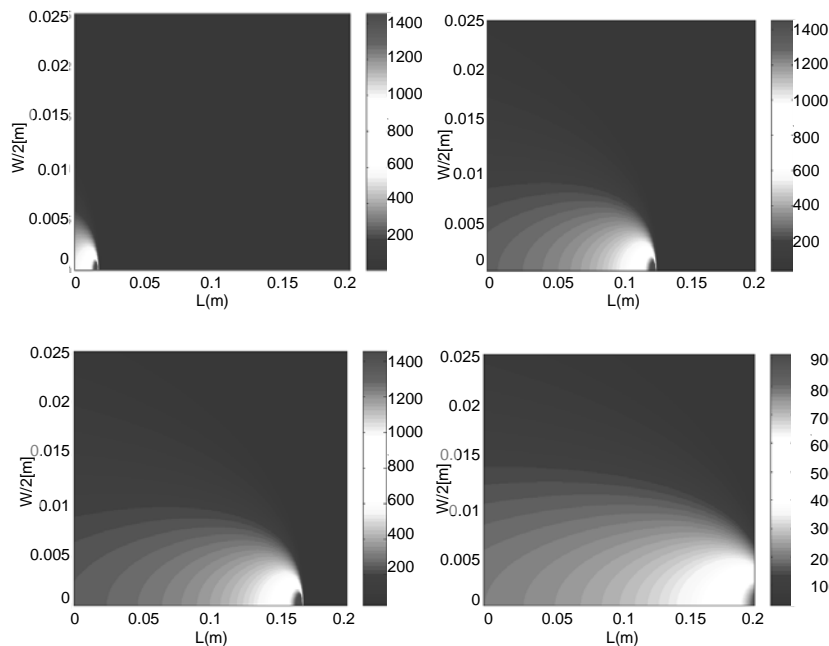

Figure 5. Resulting temperature field at the welding face at different elapsed welding times (2, 10, 20 and 25s). Estimation using model 1 and thermocouple 1.

It need be observed that the Rosenthal physical model gives good results just for temperature away from the moving heat source. This fact is due to the model not taking into account the phase change presence. Interface position of phase change is partially identified by using a pass low filter where any temperature higher than the fusion value is assumed equal to $T = T_m$. The main disadvantage of this procedure is that the position of the molten pool is dependent of the choice of the kind and place of the filter. Table 1 presents the results to the q estimation using model 1.

Table 1. Heat input estimation results using SA and model 1, P=1178W.

Thermocouple	q(W²)	η= q/P (%)
1	656	55.6
2	816	69.2
3	901	76.5
4	798	67.7

5.3. *Temperature field and radius of weld pool estimation, r (model 2).*

As mentioned before, in contrast to the previous q estimation, the unknown variable in model 2 is the fusion radius, r, and the location of the interface of phase change. In this case, an advantage of this procedure is the possibility of validation of the radius estimation, since the experimental width, L_c of weld pool will correspond to the diameter of the pool and can be obtained at the final of experiment. It means that if the weld pool is assumed circular, the estimated value of the radius, r, can be compared with the half of the value of L_c ($r = L_c/2$). The width of weld cord for a typical experimental condition was obtained using an image analyzer with an optical microscopic Neophot 21 as shown in Figure 6.
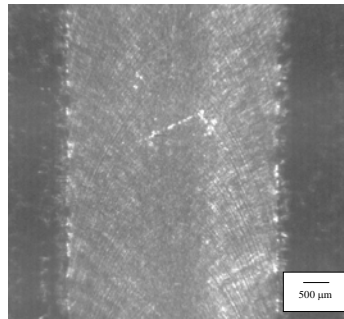

Figure 6. A weld bead from a typical experimental condition, obtained by using images from an optical microscopic, used for the width measurements.

Figure 7 shows the temperature field at the welding face at different times for thermocouple 1.
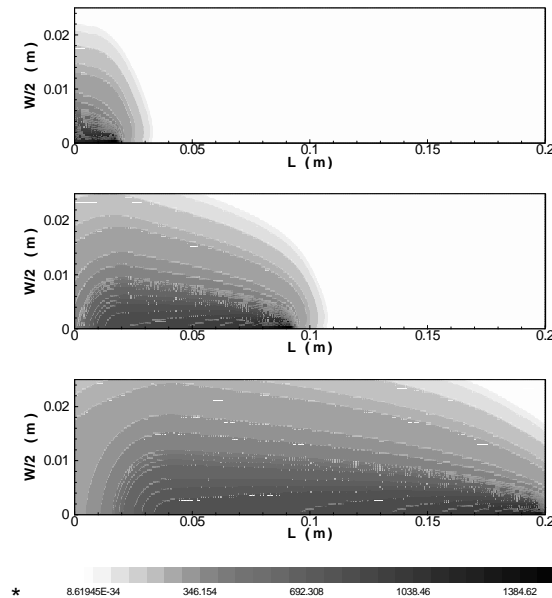

Figure 7. Estimated temperature evolution at three different elapsed times t = 2, 15 and 25 s (model 2).

The weld width determination compared with r estimation is shown in Table 2. The search interval ranges from 0.0 to $4 \cdot 10^{-3}$ m with a tolerance of $5 \cdot 10^{-5}$ m. A discrepancy less than 6.8% is obtained.

Table 2. Radius estimation obtained golden section and model 2.

Thermocouple	r (10^{-3} m)	Lc_inv (10^{-3} m)	Lc (10^{-3} m)	Relative error(%)
1	1.96	3.92	4.20	6.8
2	2.13	4.26	4.18	2.0
3	2.03	4.06	3.94	3.2
4	1.95	3.90	3.75	4.0

5.4. Comparison of results using model 1 and 2
Figures 8 to 9 present a comparison between the estimated and experimental temperatures obtained using the two models proposed.
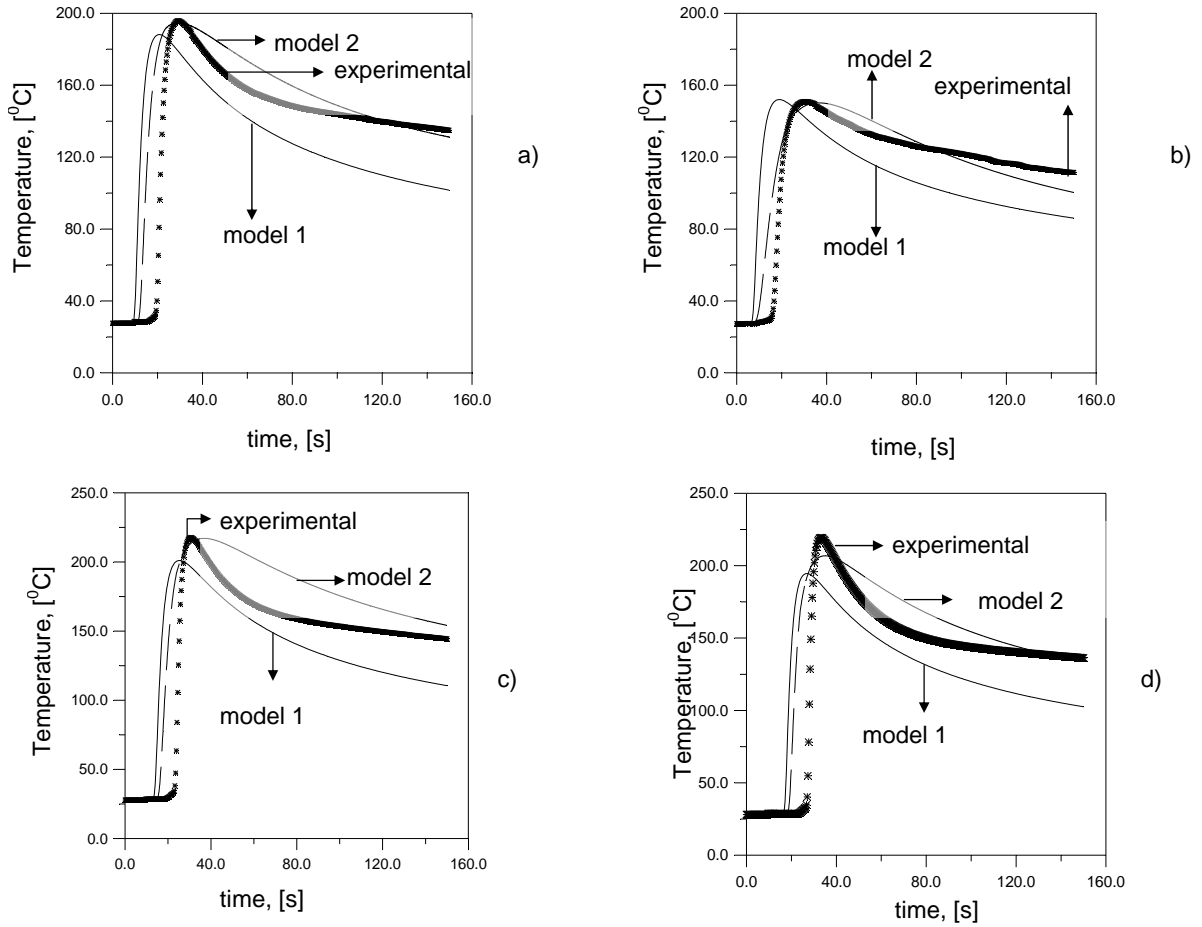

Figure 8. Comparison between the estimated and experimental temperatures obtained using the two models proposed. Thermocouples: a) 1, b) 2, c) 3 d) 4.

It can be observed that the model 2 presents results closer to the experimental evolution. This behavior can be attributed to effects like phase change and the values of thermal properties varying with temperature that are considered in this model. The effect of radiation and convection loss can be more observed at the cooling phase.

In order to obtain a better comparison among the results, quadratic error evolutions for each thermocouple are presented in the Figure 9.

Again, it can be observed that the model 2 presents better results which can be verified by the smaller values of S_T. It also can be observed that in the model 1 the maximum deviate are in the cooling phase (after 24 s) which can be justified by the absence of the heat convection and radiation effect in the Rosenthal model.
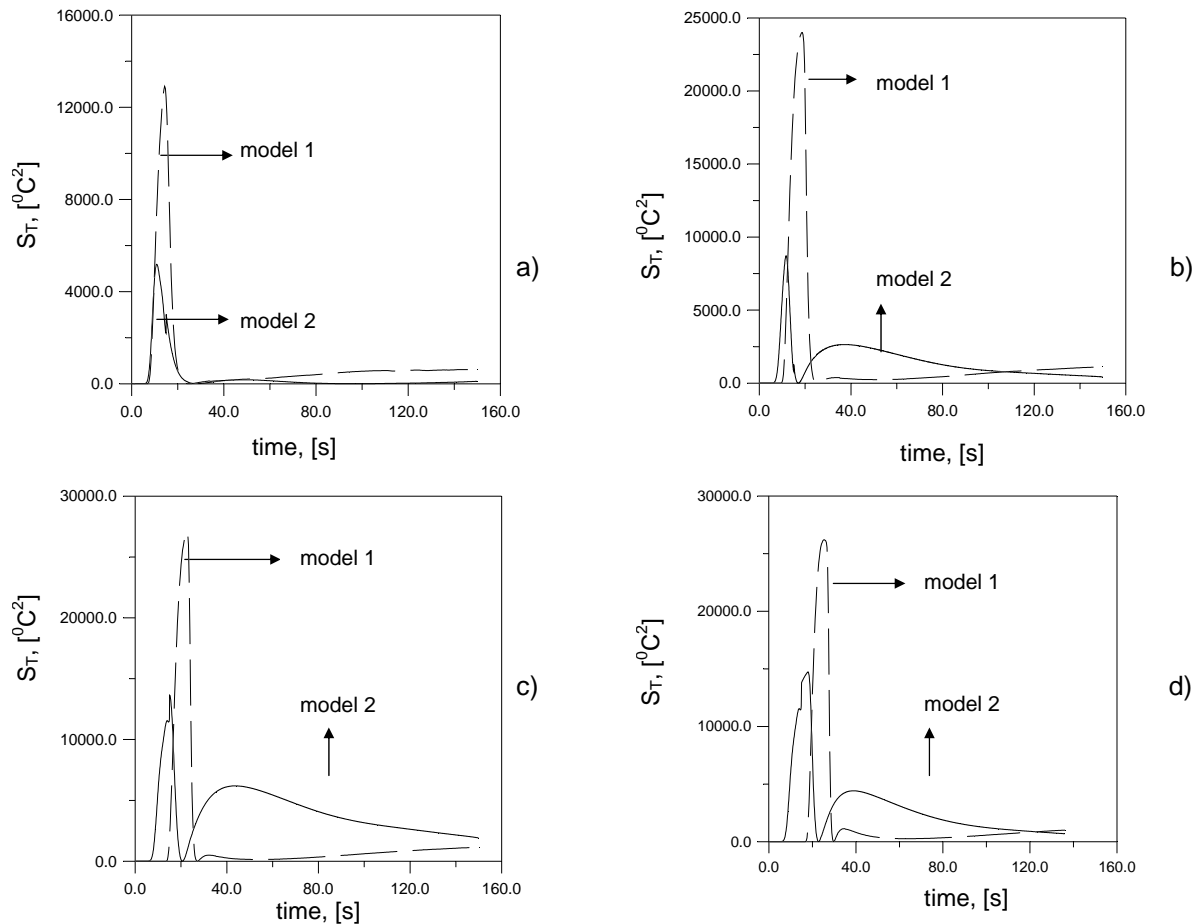
Figure 9. Objective function, S_T obtained using the two models proposed. Results obtained by using the thermocouples: a) 1, b) 2, c) 3 d) 4.

6. CONCLUSION

The circular shape assumed to the weld pool has shown to be a very good approximation for GTAW with heat source speed velocity at order of $u > 0.008333$ m/s. The deviate of the values for measured and estimated radius less than 7% has confirmed this conclusion. The physical model that consider the phase change, thermal properties varying with temperature and heat loss to the medium for convection and radiation allows the identification of thermal efficiency of fusion at each instant of the process. It can also be concluded that the transient model (model 2) presents more accurate results when compared to the simplified one (Rosenthal's model). However, if just average values are required, the use of Rosenthal model represents a very good option, since the simplified model is easy to implement and it is very inexpensive in the use of computational time consuming.

REFERENCES

1. N. Al-Khalidy, Enthalpy technique for solution of Stefan problems: application of the keyhole plasma arc welding process involving moving heat source. *Int. Comm. Heat Mass Transfer* (1995) **22,** 779-790.
2. N. Al-Khalidy, Application of optimization methods for solving inverse phase-change problems. *Num. Heat Transfer*, Part B (1997) **31**, 477-497.
3. O. M. Alifanov, Solution of an inverse problem of heat conduction by iterations methods. *J. Eng. Phys.* (1974) **26**, 471-476.
4. J.V. Beck and B. Blackwell, *Handbook of Numerical Heat Transfer*, John Wiley & Sons Inc., New York, 1988.

5. J.V. Beck, B. Blackwell and C.R. St. Clair, *Inverse Heat Conduction, Ill-posed Problems*, Wiley Interscience Publication, New York, 1985.
6. E.A. Bonifaz, Finite element analysis of heat flow in single-pass arc welds. *Welding Research Suppl.* (2000) **5,** 121s-125s.
7. K.S. Boo and H.S. Cho, Transient temperature distribution in arc welding of finite thickness plates. *Proc. Institute of Mechanical Eng.* (1990) **204**, 175-183.
8. Y. Cao, A. Faghri and W. Chang**,** A numerical analysis of stefan problems for generalized multi-dimensional phase-change structures using the enthalpy transforming model. *Int. J. Heat Mass Transfer* (1989) **32**, 1289-1298.
9. J. Crank, *Free and Moving Boundary Problems*, Claredon Press, N.Y., USA, 1984.
10. J. Goldak, M. Bibby, J. Moore and B. Patel, Computer modeling of heat flow in welds, *Metallurgical Transactions B* (1986) **17B ,** 587-600.
11. C.V. Gonçalves, *Inverse Heat Transfer Problems with Phase Change: an Welding Application*, PhD Thesis, Federal University of Uberlândia, Brazil, 2004.
12 Y. F. Hsu, B. Rubinsky, and K. Mahin, An inverse finite element method for the analysis of stationary arc welding processes. *J. Heat Transfer* (1986) **108**, 734-741.
13. S.K. Jeong and H.S. Cho, An analytical solution to predict the transient temperature distribution in filled arc welds. *Welding J.* (1997) **76,** 223-232.
14. G.H. Kraus, Thermal finite element formulation and solution versus experimental results for thin-plate gta welding. J. Heat Transfer (1986) **108**, 591-596.
15. T. Nguyen, A. Ohta, K. Matsuoka, N. Suzuki and Y. Maeda, Analytical solutions for transient temperature of semi-infinite body subjected to 3-d moving heat sources. *Welding J.* (1999) **11**, 265s-274s.
16. M.N. Ozisik, *Heat Conduction*, John Wiley & Sons, N.Y., USA, 1993.
17. S.V. Patankar, *Numerical Heat Transfer and Fluid Flow*, Hemisphere Publishing Corporation, USA, 1980.
18. D. Rosenthal, Mathematical theory of heat distribution during welding and cutting. *Welding J.* (1941) **20,** 220-234.
19. B. Rubinsky and A. Shitzer, Analytic solutions to the heat equation involving a moving boundary with applications to the change of phase problem (the inverse Stefan problem). *J. Heat Transfer* (1978) **105,** 550-554.
20. S.F.P. Saramago, E.G. Assis and V. Steffen, Simulated annealing: some applications in mechanical systems optimization. *Proc. of 20th Iberian Latin - American Cong. on Comp. Meth. in Eng.*, São Paulo, Brasil, 1999.
21. M.D. Shian and P.S. Wei, Three-dimensional analytical temperature field around the welding cavity produced by a moving distributed high-intensity beam. *J.Heat Transfer* (1993) **115,** 848-855.
22. C.R. Swaminathan, V.R. Voller, On the enthalpy-method. *Int. J. Num. Meth. Heat Fluid Flow* (1993) **3,** 233-244.
23. C.L. Tsai and C.A. Hou, Theoretical analysis of weld pool behavior in the pulsed current gtaw process. *J. Heat Transfer* (1988) **110,** 160-165.
24. G.N. Vanderplaats, *Numerical Optimization Techniques for Engineering Design*, McGraw-Hill, USA, 1999.
25. L. O. Vilarinho, *Development of Experimental and Numerical Techniques for TIG Arch Characterization*, PhD Thesis, Federal University of Uberlândia, Brazil, 2003.
26. V.R. Voller and C.Prakash, A fixed grid numerical modeling methodology for convection/diffusion mushy region phase change problems. *Int. J. Heat and Mass Transfer* (1987) **30,** 1709-1719.
27. T. Zacharia, A.H. Eraslan and D.K. Aidun, Modeling of non-Autogenous welding. *Welding Research Suppl.* (1998) **67,** 18-27.